

Centrality Dependence of π^0 and η Production at Large Transverse Momentum in $\sqrt{s_{NN}} = 200$ GeV $d + Au$ Collisions

S. S. Adler,⁵ S. Afanasiev,²⁰ C. Aidala,¹⁰ N. N. Ajitanand,⁴⁴ Y. Akiba,^{21,40} A. Al-Jamel,³⁵ J. Alexander,⁴⁴ K. Aoki,²⁵ L. Aphecetche,⁴⁶ R. Armendariz,³⁵ S. H. Aronson,⁵ R. Averbeck,⁴⁵ T. C. Awes,³⁶ V. Babintsev,¹⁷ A. Baldisseri,¹¹ K. N. Barish,⁶ P. D. Barnes,²⁸ B. Bassalleck,³⁴ S. Bathe,^{6,31} S. Batsouli,¹⁰ V. Baublis,³⁹ F. Bauer,⁶ A. Bazilevsky,^{5,41} S. Belikov,^{19,17} M. T. Bjornrdal,¹⁰ J. G. Boissevain,²⁸ H. Borel,¹¹ M. L. Brooks,²⁸ D. S. Brown,³⁵ N. Bruner,³⁴ D. Bucher,³¹ H. Buesching,^{5,31} V. Bumazhnov,¹⁷ G. Bunce,^{5,41} J. M. Burward-Hoy,^{28,27} S. Butsyk,⁴⁵ X. Camard,⁴⁶ P. Chand,⁴ W. C. Chang,² S. Chernichenko,¹⁷ C. Y. Chi,¹⁰ J. Chiba,²¹ M. Chiu,¹⁰ I. J. Choi,⁵³ R. K. Choudhury,⁴ T. Chujo,⁵ V. Cianciolo,³⁶ Y. Cobigo,¹¹ B. A. Cole,¹⁰ M. P. Comets,³⁷ P. Constantin,¹⁹ M. Csanád,¹³ T. Csörgő,²² J. P. Cussonneau,⁴⁶ D. d'Enterria,¹⁰ K. Das,¹⁴ G. David,⁵ F. Deák,¹³ H. Delagrange,⁴⁶ A. Denisov,¹⁷ A. Deshpande,⁴¹ E. J. Desmond,⁵ A. Devismes,⁴⁵ O. Dietzsch,⁴² J. L. Drachenberg,¹ O. Drapier,²⁶ A. Drees,⁴⁵ A. Durum,¹⁷ D. Dutta,⁴ V. Dzhordzhadze,⁴⁷ Y. V. Efremenko,³⁶ H. En'yo,^{40,41} B. Espagnon,³⁷ S. Esumi,⁴⁹ D. E. Fields,^{34,41} C. Finck,⁴⁶ F. Fleuret,²⁶ S. L. Fokin,²⁴ B. D. Fox,⁴¹ Z. Fraenkel,⁵² J. E. Frantz,¹⁰ A. Franz,⁵ A. D. Frawley,¹⁴ Y. Fukao,^{25,40,41} S.-Y. Fung,⁶ S. Gadrat,²⁹ M. Germain,⁴⁶ A. Glenn,⁴⁷ M. Gonin,²⁶ J. Gosset,¹¹ Y. Goto,^{40,41} R. Granier de Cassagnac,²⁶ N. Grau,¹⁹ S. V. Greene,⁵⁰ M. Grosse Perdekamp,^{18,41} H.-Å. Gustafsson,³⁰ T. Hachiya,¹⁶ J. S. Haggerty,⁵ H. Hamagaki,⁸ A. G. Hansen,²⁸ E. P. Hartouni,²⁷ M. Harvey,⁵ K. Hasuko,⁴⁰ R. Hayano,⁸ X. He,¹⁵ M. Heffner,²⁷ T. K. Hemmick,⁴⁵ J. M. Heuser,⁴⁰ P. Hidas,²² H. Hiejima,¹⁸ J. C. Hill,¹⁹ R. Hobbs,³⁴ W. Holzmann,⁴⁴ K. Homma,¹⁶ B. Hong,²³ A. Hoover,³⁵ T. Horaguchi,^{40,41,48} T. Ichihara,^{40,41} V. V. Ikonnikov,²⁴ K. Imai,^{25,40} M. Inaba,⁴⁹ M. Inuzuka,⁸ D. Isenhower,¹ L. Isenhower,¹ M. Ishihara,⁴⁰ M. Issah,⁴⁴ A. Isupov,²⁰ B. V. Jacak,⁴⁵ J. Jia,⁴⁵ O. Jinnouchi,^{40,41} B. M. Johnson,⁵ S. C. Johnson,²⁷ K. S. Joo,³² D. Jouan,³⁷ F. Kajihara,⁸ S. Kametani,^{8,51} N. Kamihara,^{40,48} M. Kaneta,⁴¹ J. H. Kang,⁵³ K. Katou,⁵¹ T. Kawabata,⁸ A. V. Kazantsev,²⁴ S. Kelly,^{9,10} B. Khachaturov,⁵² A. Khanzadeev,³⁹ J. Kikuchi,⁵¹ D. J. Kim,⁵³ E. Kim,⁴³ G.-B. Kim,²⁶ H. J. Kim,⁵³ E. Kinney,⁹ A. Kiss,¹³ E. Kistenev,⁵ A. Kiyomichi,⁴⁰ C. Klein-Boesing,³¹ H. Kobayashi,⁴¹ L. Kochenda,³⁹ V. Kochetkov,¹⁷ R. Kohara,¹⁶ B. Komkov,³⁹ M. Konno,⁴⁹ D. Kotchetkov,⁶ A. Kozlov,⁵² P. J. Kroon,⁵ C. H. Kuberg,^{1,*} G. J. Kunde,²⁸ K. Kurita,⁴⁰ M. J. Kweon,²³ Y. Kwon,⁵³ G. S. Kyle,³⁵ R. Lacey,⁴⁴ J. G. Lajoie,¹⁹ Y. Le Bornec,³⁷ A. Lebedev,^{19,24} S. Leckey,⁴⁵ D. M. Lee,²⁸ M. J. Leitch,²⁸ M. A. L. Leite,⁴² X. H. Li,⁶ H. Lim,⁴³ A. Litvinenko,²⁰ M. X. Liu,²⁸ C. F. Maguire,⁵⁰ Y. I. Makdisi,⁵ A. Malakhov,²⁰ V. I. Manko,²⁴ Y. Mao,^{38,40} G. Martinez,⁴⁶ H. Masui,⁴⁹ F. Matathias,⁴⁵ T. Matsumoto,^{8,51} M. C. McCain,¹ P. L. McGaughey,²⁸ Y. Miake,⁴⁹ T. E. Miller,⁵⁰ A. Milov,⁴⁵ S. Mioduszewski,⁵ G. C. Mishra,¹⁵ J. T. Mitchell,⁵ A. K. Mohanty,⁴ D. P. Morrison,⁵ J. M. Moss,²⁸ D. Mukhopadhyay,⁵² M. Muniruzzaman,⁶ S. Nagamiya,²¹ J. L. Nagle,^{9,10} T. Nakamura,¹⁶ J. Newby,⁴⁷ A. S. Nyanin,²⁴ J. Nystrand,³⁰ E. O'Brien,⁵ C. A. Ogilvie,¹⁹ H. Ohnishi,⁴⁰ I. D. Ojha,^{3,50} H. Okada,^{25,40} K. Okada,^{40,41} A. Oskarsson,³⁰ I. Otterlund,³⁰ K. Oyama,⁸ K. Ozawa,⁸ D. Pal,⁵² A. P. T. Palounek,²⁸ V. Pantuev,⁴⁵ V. Papavassiliou,³⁵ J. Park,⁴³ W. J. Park,²³ S. F. Pate,³⁵ H. Pei,¹⁹ V. Penev,²⁰ J.-C. Peng,¹⁸ H. Pereira,¹¹ V. Peresedov,²⁰ A. Pierson,³⁴ C. Pinkenburg,⁵ R. P. Pisani,⁵ M. L. Purschke,⁵ A. K. Purwar,⁴⁵ J. M. Qualls,¹ J. Rak,¹⁹ I. Ravinovich,⁵² K. F. Read,^{36,47} M. Reuter,⁴⁵ K. Reygers,³¹ V. Riabov,³⁹ Y. Riabov,³⁹ G. Roche,²⁹ A. Romana,^{26,*} M. Rosati,¹⁹ S. S. E. Rosendahl,³⁰ P. Rosnet,²⁹ V. L. Rykov,⁴⁰ S. S. Ryu,⁵³ B. Sahlmueller,³¹ N. Saito,^{25,40,41} T. Sakaguchi,^{8,51} S. Sakai,⁴⁹ V. Samsonov,³⁹ L. Sanfratello,³⁴ R. Santo,³¹ H. D. Sato,^{25,40} S. Sato,^{5,49} S. Sawada,²¹ Y. Schutz,⁴⁶ V. Semenov,¹⁷ R. Seto,⁶ T. K. Shea,⁵ I. Shein,¹⁷ T.-A. Shibata,^{40,48} K. Shigaki,¹⁶ M. Shimomura,⁴⁹ A. Sickles,⁴⁵ C. L. Silva,⁴² D. Silvermyr,²⁸ K. S. Sim,²³ A. Soldatov,¹⁷ R. A. Soltz,²⁷ W. E. Sondheim,²⁸ S. P. Sorensen,⁴⁷ I. V. Sourikova,⁵ F. Staley,¹¹ P. W. Stankus,³⁶ E. Stenlund,³⁰ M. Stepanov,³⁵ A. Ster,²² S. P. Stoll,⁵ T. Sugitate,¹⁶ J. P. Sullivan,²⁸ S. Takagi,⁴⁹ E. M. Takagui,⁴² A. Taketani,^{40,41} K. H. Tanaka,²¹ Y. Tanaka,³³ K. Tanida,⁴⁰ M. J. Tannenbaum,⁵ A. Taranenko,⁴⁴ P. Tarján,¹² T. L. Thomas,³⁴ M. Togawa,^{25,40} J. Tojo,⁴⁰ H. Torii,^{25,41} R. S. Towell,¹ V.-N. Tram,²⁶ I. Tserruya,⁵² Y. Tsuchimoto,¹⁶ H. Tydesjö,³⁰ N. Tyurin,¹⁷ T. J. Uam,³² J. Velkovska,⁵ M. Velkovsky,⁴⁵ V. Veszprémi,¹² A. A. Vinogradov,²⁴ M. A. Volkov,²⁴ E. Vznuzdaev,³⁹ X. R. Wang,¹⁵ Y. Watanabe,^{40,41} S. N. White,⁵ N. Willis,³⁷ F. K. Wohn,¹⁹ C. L. Woody,⁵ W. Xie,⁶ A. Yanovich,¹⁷ S. Yokkaichi,^{40,41} G. R. Young,³⁶ I. E. Yushmanov,²⁴ W. A. Zajc,^{10,†} O. Zaudtke,³¹ C. Zhang,¹⁰ S. Zhou,⁷ J. Zimányi,^{22,*} L. Zolin,²⁰ X. Zong,¹⁹ and H. W. vanHecke²⁸

(PHENIX Collaboration)

¹Abilene Christian University, Abilene, Texas 79699, USA

²Institute of Physics, Academia Sinica, Taipei 11529, Taiwan

- ³Department of Physics, Banaras Hindu University, Varanasi 221005, India
⁴Bhabha Atomic Research Centre, Bombay 400 085, India
⁵Brookhaven National Laboratory, Upton, New York 11973-5000, USA
⁶University of California-Riverside, Riverside, California 92521, USA
⁷China Institute of Atomic Energy (CIAE), Beijing, People's Republic of China
⁸Center for Nuclear Study, Graduate School of Science, University of Tokyo, 7-3-1 Hongo, Bunkyo, Tokyo 113-0033, Japan
⁹University of Colorado, Boulder, Colorado 80309, USA
¹⁰Columbia University, New York, New York 10027 and Nevis Laboratories, Irvington, New York 10533, USA
¹¹Dapnia, CEA Saclay, F-91191, Gif-sur-Yvette, France
¹²Debrecen University, H-4010 Debrecen, Egyetem tér 1, Hungary
¹³ELTE, Eötvös Loránd University, H-1117 Budapest, Pázmány P. s. 1/A, Hungary
¹⁴Florida State University, Tallahassee, Florida 32306, USA
¹⁵Georgia State University, Atlanta, Georgia 30303, USA
¹⁶Hiroshima University, Kagamiyama, Higashi-Hiroshima 739-8526, Japan
¹⁷IHEP Protvino, State Research Center of Russian Federation, Institute for High Energy Physics, Protvino, 142281, Russia
¹⁸University of Illinois at Urbana-Champaign, Urbana, Illinois 61801, USA
¹⁹Iowa State University, Ames, Iowa 50011, USA
²⁰Joint Institute for Nuclear Research, 141980 Dubna, Moscow Region, Russia
²¹KEK, High Energy Accelerator Research Organization, Tsukuba, Ibaraki 305-0801, Japan
²²KFKI Research Institute for Particle and Nuclear Physics of the Hungarian Academy of Sciences (MTA KFKI RMKI), H-1525 Budapest 114, POBox 49, Budapest, Hungary
²³Korea University, Seoul, 136-701, Korea
²⁴Russian Research Center "Kurchatov Institute", Moscow, Russia
²⁵Kyoto University, Kyoto 606-8502, Japan
²⁶Laboratoire Leprince-Ringuet, Ecole Polytechnique, CNRS-IN2P3, Route de Saclay, F-91128, Palaiseau, France
²⁷Lawrence Livermore National Laboratory, Livermore, California 94550, USA
²⁸Los Alamos National Laboratory, Los Alamos, New Mexico 87545, USA
²⁹LPC, Université Blaise Pascal, CNRS-IN2P3, Clermont-Fd, 63177 Aubiere Cedex, France
³⁰Department of Physics, Lund University, Box 118, SE-221 00 Lund, Sweden
³¹Institut für Kernphysik, University of Muenster, D-48149 Muenster, Germany
³²Myongji University, Yongin, Kyonggido 449-728, Korea
³³Nagasaki Institute of Applied Science, Nagasaki-shi, Nagasaki 851-0193, Japan
³⁴University of New Mexico, Albuquerque, New Mexico 87131, USA
³⁵New Mexico State University, Las Cruces, New Mexico 88003, USA
³⁶Oak Ridge National Laboratory, Oak Ridge, Tennessee 37831, USA
³⁷IPN-Orsay, Université Paris Sud, CNRS-IN2P3, BP1, F-91406, Orsay, France
³⁸Peking University, Beijing, People's Republic of China
³⁹PNPI, Petersburg Nuclear Physics Institute, Gatchina, Leningrad region, 188300, Russia
⁴⁰RIKEN (The Institute of Physical and Chemical Research), Wako, Saitama 351-0198, JAPAN
⁴¹RIKEN BNL Research Center, Brookhaven National Laboratory, Upton, New York 11973-5000, USA
⁴²Universidade de São Paulo, Instituto de Física, Caixa Postal 66318, São Paulo CEP05315-970, Brazil
⁴³System Electronics Laboratory, Seoul National University, Seoul, South Korea
⁴⁴Chemistry Department, Stony Brook University, Stony Brook, SUNY, New York 11794-3400, USA
⁴⁵Department of Physics and Astronomy, Stony Brook University, SUNY, Stony Brook, New York 11794, USA
⁴⁶SUBATECH (Ecole des Mines de Nantes, CNRS-IN2P3, Université de Nantes) BP 20722-44307, Nantes, France
⁴⁷University of Tennessee, Knoxville, Tennessee 37996, USA
⁴⁸Department of Physics, Tokyo Institute of Technology, Oh-okayama, Meguro, Tokyo 152-8551, Japan
⁴⁹Institute of Physics, University of Tsukuba, Tsukuba, Ibaraki 305, Japan
⁵⁰Vanderbilt University, Nashville, Tennessee 37235, USA
⁵¹Waseda University, Advanced Research Institute for Science and Engineering, 17 Kikui-cho, Shinjuku-ku, Tokyo 162-0044, Japan
⁵²Weizmann Institute, Rehovot 76100, Israel
⁵³Yonsei University, IPAP, Seoul 120-749, Korea

(Received 23 October 2006; published 24 April 2007)

The dependence of transverse momentum spectra of neutral pions and η mesons with $p_T < 16$ GeV/c and $p_T < 12$ GeV/c, respectively, on the centrality of the collision has been measured at midrapidity by the PHENIX experiment at the BNL Relativistic Heavy Ion Collider (RHIC) in $d + Au$ collisions at $\sqrt{s_{NN}} = 200$ GeV. The measured yields are compared to those in $p + p$ collisions at the same $\sqrt{s_{NN}}$ scaled by the number of underlying nucleon-nucleon collisions in $d + Au$. At all centralities, the yield ratios show no suppression, in contrast to the strong suppression seen for central Au + Au collisions at RHIC. Only a weak p_T and centrality dependence can be observed.

DOI: 10.1103/PhysRevLett.98.172302

PACS numbers: 25.75.Dw

High-energy nucleus-nucleus collisions provide the opportunity to study strongly interacting matter at very high energy densities where Quantum Chromodynamics (QCD) predicts a transition from normal nuclear matter to a deconfined system of quarks and gluons, the Quark-Gluon Plasma (QGP) [1]. At the Relativistic Heavy Ion Collider (RHIC), the energy density is well in excess of the critical energy density that is expected for this transition [2]. One of the most intriguing results observed at RHIC so far is the suppression of hadrons with high transverse momentum (p_T) in central (head-on) Au + Au collisions. The hadron yield at high p_T is a factor of 5 less than expected from $p + p$ collisions scaled by the number of corresponding nucleon-nucleon collisions [3]. Such suppression was predicted as an effect of parton energy loss in the medium generated in the collisions [4,5]. A control experiment of $d + Au$ collisions, where no medium is produced in the final state of the collision, showed no indication of hadron suppression at midrapidity [6], ruling out strong initial-state effects (final-state energy loss in the cold nucleus is generally expected to be small) as the cause for the suppression in Au + Au. For a better understanding of the medium effects at work in Au + Au, however, it is crucial to explore the exact role initial-state effects play in the modification of high- p_T particle production at RHIC.

Initial-state nuclear effects include p_T broadening, shadowing, and gluon saturation. The p_T broadening, often called Cronin effect [7], is an enhancement of the particle yield at intermediate p_T , which is often attributed to multiple soft parton scatterings before a hard interaction of the parton [8,9]. Shadowing is an apparent depletion of the structure function in the nucleus at small Bjorken x ($x \leq 10^{-2}$) [10] with (in some models) a corresponding enhancement at intermediate x ($x \sim 5 \times 10^{-2}$) called antishadowing. This is not well understood, but usually attributed to coherence effects or to gluon saturation. Gluon saturation refers to the nonlinear dynamics of gluons at small x where, due to the large densities, they tend to fuse rather than split. The Color Glass Condensate (CGC) model is a classical description of this saturation effect. In this picture, particle production at moderate p_T originally was predicted to be suppressed in central $d + Au$ collisions at RHIC [11]. In recent CGC models, a Cronin enhancement can also be reproduced with a suitable choice of initial-state parameters [12].

One established way to test the contribution of different initial- and final-state nuclear effects is the study of the centrality dependence of particle production at high p_T . Initial state and medium effects are strongest in central collisions. In Au + Au collisions, a strong dependence of the suppression of high- p_T hadrons on the centrality of the collision has been observed [13–15]; the suppression weakens going to peripheral collisions and finally disap-

pears. This can be compared to the centrality dependence of (initial-state) hadron production in $d + Au$. The yield of nonidentified charged hadrons in $d + Au$ collisions with $p_T < 6$ GeV/ c was found to be increasingly enhanced going from peripheral to central collisions [16], mainly attributed to the influence of (anti)protons [17]. At high p_T , the baryon contribution to the yield of unidentified charged hadrons is expected to become small, and instead the yield is dominated by charged pions [2]. All this sparks paramount interest in the centrality dependence of neutral pion (π^0) production especially as it can be measured up to very high p_T where particle production is truly perturbative. Furthermore, the high- p_T measurement of an additional identified particle like the eta meson (η), with 4 times the mass of the pion, may shed light on the question to what extent the particle-species dependence of the suppression (enhancement) observed in Au + Au ($d + Au$) depends on the number of constituent quarks rather than on the mass of the particle [18,19].

In this Letter, we present measurements by the PHENIX experiment [20] on the production of π^0 and η in $p + p$ and $d + Au$ collisions at $\sqrt{s_{NN}} = 200$ GeV. The data provide the first measurement of neutral mesons in $d + Au$ collisions at midrapidity as a function of the centrality of the collision. The π^0 measurements described in this Letter are similar to the analysis of minimum bias $d + Au$ data in [6] but are based on an improved data set that allows the study of the particle production for different selections of the centrality of the collision. A more detailed description of the η analysis can be found in [21].

π^0 and η are measured by the PHENIX electromagnetic calorimeter (EMCal) via the $\pi^0 \rightarrow \gamma\gamma$ and $\eta \rightarrow \gamma\gamma$ decay. The EMCal consists of six lead scintillator (PbSc) and two lead glass (PbGl) sectors, each located at a radial distance of ~ 5 m from the beam axis. The detector covers a pseudorapidity range of $|\eta| \leq 0.35$ and an azimuthal angle of $\Delta\phi = \pi$. The EMCal granularity is $\Delta\eta \times \Delta\phi \approx 0.011 \times 0.011$ for the PbSc and 0.008×0.008 for the PbGl. The data sets from PbSc and PbGl are analyzed separately and combined for the final results. The energy calibration for the EMCal is obtained from beam tests, cosmic rays, and minimum ionizing energy peaks of charged hadrons. In a recent improvement of the calibration, the EMCal is calibrated by the invariant mass distribution of neutral pions for each of the 24768 readout channels separately. The uncertainty on the energy scale is 1.2%.

The data used in this analysis were recorded in 2002–2003 (RHIC Run-3) under two different trigger conditions. 25.2×10^6 and 58.3×10^6 minimum bias events were analyzed for $p + p$ and $d + Au$ collisions, respectively. Minimum bias (MB) events are triggered by the Beam-Beam Counters (BBC) [20] ($|\eta| = 3.0\text{--}3.9$) and require a vertex position along the beam axis within $|z| < 30$ cm.

The minimum bias trigger accepts $(88 \pm 4)\%$ of all inelastic $d + \text{Au}$ collisions that satisfy the vertex condition. This corresponds to $1.99 \text{ b} \pm 5.2\%$, the measured fraction of the total $d + \text{Au}$ inelastic cross section, determined using photo-dissociation of the deuteron [22]. In $p + p$, this trigger measures $23.0 \text{ mb} \pm 9.7\%$ of the $p + p$ inelastic cross section. The measured particle yields are corrected for the $p + p$ MB trigger bias [23]: the MB trigger measures only $(79 \pm 2)\%$ of high- p_T particles. In $d + \text{Au}$ collisions, this fraction varies from 85% to 100% from peripheral to central collisions; here the uncertainty is $\sim 3\%$. The second data sample was collected with a high- p_T photon trigger in the EMCal in addition to the MB trigger requirement in order to extend the measurement to higher p_T . This trigger requires a photon of $p_T > 1.4(1.4) \text{ GeV}$ and $p_T > 2.5(3.5) \text{ GeV}$ for PbSc (PbGl) and for $p + p$ and $d + \text{Au}$ collisions, respectively. We analyzed 45.1×10^6 (19.5×10^6) events in $p + p$ ($d + \text{Au}$) under this trigger condition. The sampled integrated luminosity was 216 nb^{-1} for $p + p$ and 1.5 nb^{-1} for $d + \text{Au}$. (In $d + \text{Au}$, that corresponds to an integrated nucleon-nucleon luminosity of 590 nb^{-1}).

The division of $d + \text{Au}$ collisions in different centrality classes is based on the charge deposited in the backward BBC ($-3.9 < \eta < -3.0$), i.e., in the Au beam direction. For each centrality class, the corresponding average nuclear overlap function $\langle T_{AB} \rangle$ (compare Eq. (1)) is calculated using a Glauber Monte Carlo model and simulations of the BBC, taking into account its limited efficiency for peripheral collisions. For the four centrality classes (0–20%, 20–40%, 40–60%, and 60–88%) used in this analysis, the $\langle T_{AB} \rangle$ values are (0.365 ± 0.024) , (0.252 ± 0.017) , (0.165 ± 0.014) , and $(0.073 \pm 0.007) \text{ mb}^{-1}$. The corresponding number of collisions can be calculated as $\langle N_{\text{coll}} \rangle = \sigma_{\text{inel}}^{pp} \times \langle T_{AB} \rangle$ with $\sigma_{\text{inel}}^{pp} = 42.2 \text{ mb}$.

Photon candidates in the EMCal are selected by applying particle identification (PID) cuts based on the shower profile in the detector. To determine the yields of π^0 and η , the invariant mass of all photon pairs with an energy asymmetry $|E_1 - E_2|/(E_1 + E_2) < 0.7$ in a given p_T bin is calculated. After subtraction of the combinatorial back-

ground, the invariant mass distribution is integrated around the particle mass peak [13]; the integration window reflects thereby the p_T dependence of the mass peak position and width. The combinatorial background is determined by pairing photons from different events with similar centrality (for $d + \text{Au}$) and vertex. In this analysis, the signal-to-background ratio for high- p_T π^0 is about 25 and 13 at $p_T = 4 \text{ GeV}/c$ in $p + p$ and central $d + \text{Au}$ collisions, respectively. It decreases to 7 and 2 at $p_T = 2 \text{ GeV}/c$. For η , this ratio is about 2 at $p_T = 8 \text{ GeV}/c$, decreasing to 0.3 ($p + p$) and 0.2 (central $d + \text{Au}$) at $p_T = 3 \text{ GeV}/c$. The raw spectra are corrected for trigger efficiency, acceptance, and reconstruction efficiency. This includes dead areas, the influence of energy resolution, analysis cuts, the peak extraction window, and photon conversion. The corrections are determined using Monte Carlo simulations. Because of the fine granularity of the calorimeter, occupancy effects are negligible. Furthermore, the π^0 spectra are corrected at $p_T > 10 \text{ GeV}/c$ ($15 \text{ GeV}/c$) for two-photon merging effects in the PbSc (PbGl), studied in Monte Carlo simulations and confirmed with test beam data [24]. Finally, a correction in the π^0 and η yields to account for the true mean value of each p_T bin is applied to the steeply falling spectra. For $p_T < 3.5(3.0) \text{ GeV}/c$, the $p + p$ π^0 (η) spectrum is calculated from the minimum bias data sample; above this threshold, the high- p_T triggered sample is used. In $d + \text{Au}$, this transition is made at $p_T = 4.5$ and $3.5 \text{ GeV}/c$ for π^0 and η , respectively.

The main contributions to the systematic uncertainty on the $p + p$ and $d + \text{Au}$ spectra are given in Table I for π^0 and η . Most uncertainties are identical for $p + p$ and $d + \text{Au}$; only the uncertainty on the peak extraction is slightly larger in $d + \text{Au}$. Category (d) includes uncertainties on the EMCal global energy scale and nonlinearity. The uncertainties in (d) and (e) are partially correlated. All others are uncorrelated and added in quadrature to get the total uncertainty.

The fully corrected p_T distributions of π^0 and η are shown in Fig. 1. The top panels show the invariant yield in $d + \text{Au}$ collisions for four centrality bins scaled for clarity by the factors indicated. The bottom panels show the

TABLE I. Main systematic uncertainties in % on π^0 and η spectra. The uncertainties are given for PbSc (PbGl). The normalization uncertainties of 9.7% for the $p + p$ and 5.2% for the $d + \text{Au}$ cross section as well as the MB-trigger-bias uncertainty of $\sim 3\%$ for the centrality-selected yields are not listed.

meson [p_T (GeV/c)]	π^0 [2]	π^0 [15]	η [3]	η [10]
(a) peak extraction	2.7(2.7)	2.0(2.0)	14(14)	6.0(6.0)
(b) geom. accept.	3.5(3.5)	3.5(3.5)	4.5(4.5)	4.5(4.5)
(c) π^0 reconstr. eff.	0.7(0.7)	4.0(4.0)	0.7(0.7)	3.6(3.6)
(d) energy scale	5.0(5.0)	11.4(11.4)	5.0(5.0)	9.4(9.4)
(e) merging corr.	...	5.9(2.1)
Total	6.7(6.7)	17.0(12.9)	15.5(15.5)	12.6(12.6)

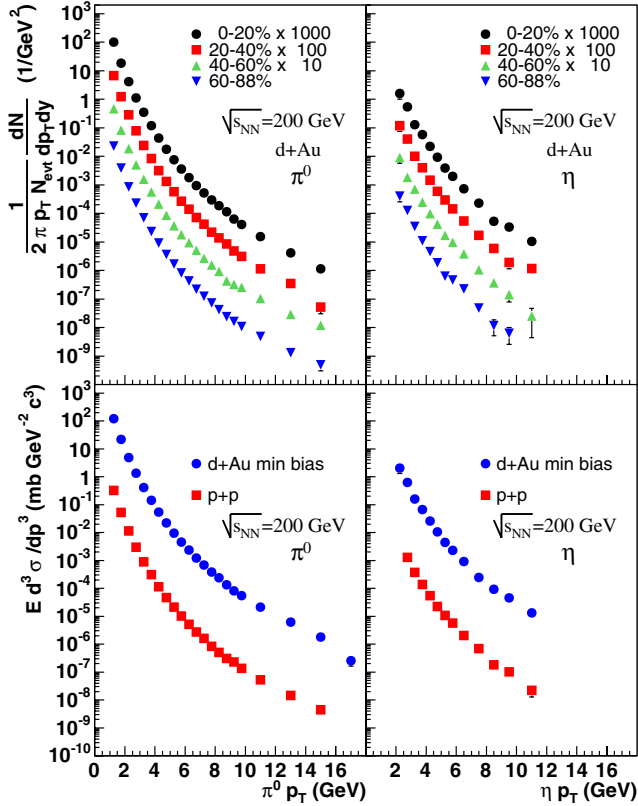


FIG. 1 (color online). Top: invariant yields at midrapidity for π^0 (left) and η (right) in $d + Au$ collisions as a function of p_T for different selections of the centrality of the collision. Bottom: invariant cross section at midrapidity for π^0 (left) and η (right) in $p + p$ and $d + Au$ collisions as a function of p_T .

invariant cross section in $p + p$ and $d + Au$ collisions. The improved data set allows the study of π^0 (η) production up to 18(12) GeV/c, the highest p_T values measured for identified particles in $p + A$ ($d + A$) collisions. For the first time, the invariant cross section for π^0 and η in $d + Au$ collisions has been measured at this energy. The π^0 result in $p + p$ agrees with the previous measurement at $\sqrt{s_{NN}} = 200$ GeV [23] within statistical uncertainties, and confirms the agreement with pQCD within the uncertainty of the calculation. Therefore, the $p + p$ cross section can be used as a well-understood reference for the production in $d + A$ and $Au + Au$ collisions.

To quantify nuclear medium effects at high p_T , it is customary to use the *nuclear modification factor* which is given by the ratio of the invariant $d + Au$ yield to the invariant $p + p$ cross section [13] scaled by $\langle T_{AB} \rangle$:

$$R_{AB}(p_T) = \frac{d^2 N_{AB}^{\pi^0} / dy dp_T}{\langle T_{AB} \rangle d^2 \sigma_{pp}^{\pi^0} / dy dp_T}. \quad (1)$$

The average nuclear overlap function $\langle T_{AB} \rangle$, averaged over the respective impact parameter range, is determined solely by the density distribution of the nucleons in the nuclei A and B and the impact parameter.

Figure 2 shows the nuclear modification factor $R_{dA}(p_T)$ for π^0 and η in $d + Au$ collisions at $\sqrt{s_{NN}} = 200$ GeV for four different centrality selections and for minimum bias events. As the $p + p$ and $d + Au$ measurements are both made in the same year, many of the systematic errors associated with detector performance are nearly identical, and the corresponding systematic errors in the comparison are negligible. Within systematic errors, $R_{dA}(p_T)$ for π^0 and η is ≈ 1 in all centrality bins, and only a weak p_T dependence can be seen. In order to check the absolute normalization systematics, we can also calculate $R_{dA}(p_T)$ using the inelastic cross section measured through photodissociation of the deuteron. This constitutes an important cross check. It replaces the systematic uncertainties of the BBC efficiency and $\langle T_{AB} \rangle$, which are determined by model calculations, by the uncertainty of the cross section measurement of similar size. The resulting $R_{dA}(p_T)$ is 9.8% larger than that obtained from the minimum bias yield, consistent within 1.5σ .

Though very different in mass, η and π^0 show a similar, weak centrality dependence of $R_{dA}(p_T)$ over the measured p_T range. These results do not show the significant enhancement seen for protons where the proton R_{AA} is substantially larger than that of pions in the intermediate p_T ($2 \text{ GeV}/c < p_T < 4 \text{ GeV}/c$) region [17]. The π^0 data exhibit small shape variations with centrality that may be due to initial-state effects including shadowing and multiple scattering. Possible Cronin enhancements in the intermediate p_T region due to initial-state multiple scattering or antishadowing are not more than 10% around 4 GeV/c. At low p_T ($p_T < 3 \text{ GeV}/c$), the drop towards smaller R_{dA} is consistent with analogous measurements for charged pions [17] and is usually attributed to a change to a regime of soft physics (N_{part} scaling) at the smallest p_T values. At the largest p_T values measured ($p_T > 9 \text{ GeV}/c$), the most central π^0 result hints at a small suppression, though this is only a ~ 1.7 sigma effect.

In conclusion, we have presented the first study of the centrality dependence of π^0 and η production at midrapidity in $d + Au$ collisions at $\sqrt{s_{NN}} = 200$ GeV. Transverse momentum spectra up to $p_T = 18$ and 12 GeV/c have been measured for π^0 and η , respectively. The invariant yield per nucleon-nucleon collision is compared to that in $p + p$ collisions measured at the same $\sqrt{s_{NN}}$. The strong suppression observed for π^0 production at high p_T in central Au-Au collisions is not seen for $d + Au$ in any centrality: Within systematic errors, $R_{dA}(p_T)$ is ≈ 1 in all centrality bins. A weak centrality dependence of the shape of R_{dA} versus p_T is seen, presumably due to initial-state effects. A possible Cronin enhancement is substantially smaller than the $R_{dA} \geq 1.9$ that corresponds to results from lower energy measurements [7,25]. Within systematic errors, R_{dA} for π^0 and η agree well, giving no indication for cold nuclear matter effects having a mass dependence. Since nuclear modifications in $d + Au$ are

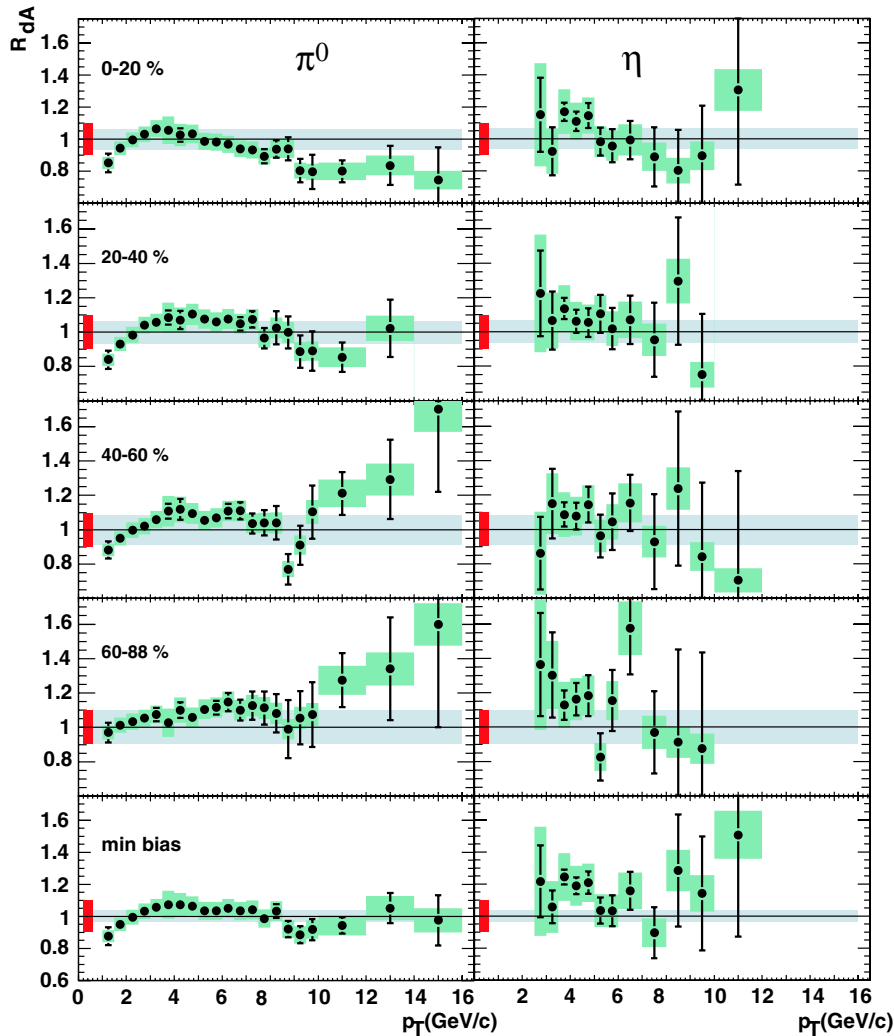


FIG. 2 (color online). Nuclear modification factor R_{dA} for π^0 and η in different centrality selections and min. bias data at midrapidity. The bands around the data points show systematic errors which can vary with p_T . The shaded bands around unity indicate the $\langle T_{AB} \rangle$ uncertainty, and the small bands on the left side of the data points indicate the normalization uncertainty due to the $p + p$ reference.

small even in the most central collisions where initial-state effects are expected to be largest, we conclude that initial-state effects in Au + Au must be small as well, and therefore the large suppression seen in Au + Au must be mostly due to medium effects.

We thank the staff of the Collider-Accelerator and Physics Departments at BNL for their vital contributions. We acknowledge support from the Department of Energy and NSF (U.S.A.), MEXT and JSPS (Japan), CNPq and FAPESP (Brazil), NSFC (China), IN2P3/CNRS, CEA, and ARMINES (France), BMBF, DAAD, and AvH (Germany), OTKA (Hungary), DAE and DST (India), ISF (Israel), KRF and KOSEF (Korea), RMIST, RAS, and RMAE (Russia), VR and KAW (Sweden), U.S. CRDF for the FSU, US-Hungarian NSF-OTKA-MTA, and US-Israel BSF.

*Deceased

†PHENIX Spokesperson: zajc@nevis.columbia.edu

- [1] J. W. Harris and B. Müller, *Annu. Rev. Nucl. Part. Sci.* **46**, 71 (1996).
- [2] K. Adcox *et al.* (PHENIX), *Nucl. Phys. A* **757**, 184 (2005).
- [3] K. Adcox *et al.* (PHENIX), *Phys. Rev. Lett.* **88**, 022301 (2001).
- [4] J. D. Bjorken, Fermilab, Report No. FERMILAB-PUB-82-059-THY, 1982.
- [5] R. Baier, D. Schiff, and B. G. Zakharov, *Ann. Rev. Nucl. Part. Sci.* **50**, 37 (2000).
- [6] S. S. Adler *et al.* (PHENIX), *Phys. Rev. Lett.* **91**, 072303 (2003).
- [7] J. W. Cronin *et al.*, *Phys. Rev. D* **11**, 3105 (1975).
- [8] I. Vitev, *Phys. Lett. B* **562**, 36 (2003).
- [9] A. Accardi and M. Gyulassy, *Phys. Lett. B* **586**, 244 (2004).
- [10] M. Arneodo, *Phys. Rep.* **240**, 301 (1994).
- [11] D. Kharzeev, E. Levin, and L. McLerran, *Phys. Lett. B* **561**, 93 (2003).
- [12] D. Kharzeev, Y. V. Kovchegov, and K. Tuchin, *Phys. Rev. D* **68**, 094013 (2003).
- [13] S. S. Adler *et al.* (PHENIX), *Phys. Rev. Lett.* **91**, 072301 (2003).

- [14] S. S. Adler *et al.* (PHENIX), Phys. Rev. C **69**, 034910 (2004).
- [15] J. Adams *et al.* (STAR), Phys. Rev. Lett. **91**, 172302 (2003).
- [16] S. S. Adler *et al.* (PHENIX), High p_T charged centrality dependence and h/π^0 ratio in $d + Au$ collisions (to be published).
- [17] S. S. Adler *et al.* (PHENIX), Phys. Rev. C **74**, 024904 (2006).
- [18] S. S. Adler *et al.* (PHENIX), Phys. Rev. C **72**, 014903 (2005).
- [19] R. C. Hwa and C. B. Yang, Phys. Rev. Lett. **93**, 082302 (2004).
- [20] K. Adcox *et al.* (PHENIX), Nucl. Instrum. Methods Phys. Res., Sect. A **499**, 469 (2003).
- [21] S. S. Adler (PHENIX), Phys. Rev. C **75**, 024909 (2007).
- [22] S. N. White, AIP Conf. Proc. **792**, 527 (2005).
- [23] S. S. Adler *et al.* (PHENIX), Phys. Rev. Lett. **91**, 241803 (2003).
- [24] G. David *et al.*, IEEE Trans. Nucl. Sci. **47**, 1982 (2000).
- [25] A. L. S. Angelis *et al.* (BCMOR), Phys. Lett. B **185**, 213 (1987).